Drug Design, Development and Therapy

Dovepress

open access to scientific and medical research

Open Access Full Text Article

ORIGINAL RESEARCH

Alginate Suppresses Liver Fibrosis Through the Inhibition of Nuclear Factor-κB Signaling

This article was published in the following Dove Press journal:
Drug Design, Development and Therapy

Ziqiang Xia[1]
Li Ding[1]
Juzeng Zheng[1]
Yilun Xu[1]
Wenyi Jin[1]
Xiong Sheng[2,3]
Jinming Wu[1]

[1]Department of Gastroenterology, The First Affiliated Hospital of Wenzhou Medical University, Wenzhou 325000, People's Republic of China; [2]Department of Infectious Diseases, The First Affiliated Hospital of Jiaxing College, Jiaxing 314000, People's Republic of China; [3]Department of Infectious Diseases, The First Hospital of Jiaxing, Jiaxing 314000, People's Republic of China

Purpose: Liver fibrosis (or liver scarring) is a causative factor for hepatitis, cirrhosis and hepatocellular carcinoma (HCC). Alginate (Agn) isolated from brown algae is known to slow the proliferation of fibroblasts, through the mechanisms of these effects remain undefined. This study explored the benefits of Agn on hepatic health and its associated mechanism(s) of action in hepatic stellate cells (HSC-T6s).

Materials and Methods: To assess the effects of Agn, HSC-T6s were treated with PDGF and cell proliferation, colony formation, cell migration, cell invasiveness and apoptosis were assessed. Rat models of liver fibrosis were produced through 12-week injections of intraperitoneal (IP) carbon tetrachloride (CCl_4). Rats were Agn-treated from weeks 8 to 12, and liver damage was assessed through Masson's and H

Materials and Methods: & E staining. Gene expression profiles were assayed via RT-PCR, Western blot and commercial ELISA kits.

Results: Agn reduced the proliferation of HSC-T6s and increased apoptotic rates through the downregulation of the Bcl-2:Bax ratio. Agn also inhibited the invasion and migration of HSC-T6s, prevented ECM deposition, and reduced the occurrence of liver fibrosis in rat models. Agn also prevented IκBα and p65 phosphorylation.

Conclusion: Agn prevents liver fibrosis through its attenuation of HSC activation and division through the suppression of NF-κB in in vitro and animal models. This highlights how the clinical use of Agn can prevent hepatic fibrosis.

Keywords: liver fibrosis, cell proliferation, alginate, apoptosis, NF-κB

Introduction

Fibrosis is the first stage of liver scarring, which during later stages progresses to liver cirrhosis. Liver fibrosis encompasses a wound a response to hepatic injury caused by autoimmune hepatitis, biliary obstruction, iron overload, nonalcoholic fatty liver disease, including nonalcoholic fatty liver (NAFL) and nonalcoholic steatohepatitis (NASH), viral hepatitis B and C, and alcoholic liver disease. The most common cause of liver fibrosis is nonalcoholic fatty liver disease (NAFLD), followed by alcoholic liver disease as a response to chronic alcohol abuse.[1] Liver fibrosis can be reversed through medical intervention[2] and the WHO reports that liver cirrhosis causes ~170,000 deaths in Europe alone each year.[3] Elevated levels of extracellular matrix (ECM) deposition are a key feature of liver fibrosis. In the resting state, hepatic stellate cells (HSC) can be induced to form myofibroblasts that produce large levels of ECM.[4] Inhibiting the division and activity of HSCs prevents extracellular matrix deposition and can reduce liver fibrosis.

Numerous molecules have protective effects on the liver. Antioxidants including vitamin E, lecithin and silymarin inhibit hepatocyte apoptosis and HSC activation,

Correspondence: Xiong Sheng
Department of Infectious Diseases, The First Affiliated Hospital of Jiaxing College, Jiaxing 314000, People's Republic of China
Tel +8613738262938
Fax +8615858827358
Email 783532291@qq.com

Jinming Wu
Department of Gastroenterology, The First Affiliated Hospital of Wenzhou Medical University, Wenzhou 325000, People's Republic of China
Tel +8613587694167
Fax +8615157785663
Email wzfydw@163.com

submit your manuscript | www.dovepress.com
DovePress
http://doi.org/10.2147/DDDT.S233665

thus reducing liver fibrosis.[5] Thiazolindiones as PPARγ ligands, inhibit the activation of HSCs and play a protective role during hepatic fibrosis.[6] Colchicine protects the liver mainly through anti–inflammatory effect.[7] Other natural molecules can also treat liver fibrosis by inhibiting TGF-β, NF-κB and PI3K-AKT signaling pathways.

NF-κB promotes hepatic damage, fibrosis and subsequent Hepatocellular Carcinoma (HCC).[8] Blocking NF-κB can increase HSC apoptosis and prevent liver damage.[9] In unstimulated cells, NF-κB dimerizes with IκBα, IκBβ and IκBε and is inactive. Upon IκB degradation, NF-κB is transcriptionally activated and binds DNA to enhance Bcl-2 transcription.[10] NF-κB is thus a critical regulator of HSC mediated liver fibrosis.

According to Traditional Chinese Medicine (TCM), the Liver is responsible for the smooth flow of emotions in addition to Qi and blood, and is a key target for therapeutic intervention. Alginate (Agn) is a water-soluble polysaccharide isolated from brown algae cytoderms that is a linear copolymer consisting of 1,4-L-glucuronic acid and 1,4-D-mannuronic acid.[11,12] Since its discovery, Agn has been used for chemical, food and biochemistry applications.[13–15] Due to its anti–viral,[16] immune,[17] anti-radiation,[18] anti-coagulation,[19] anti-oxidant,[20] anti-cancer[21] and lipid-lowering properties.[22] Agn slows the proliferation of epithelial liver cells, cancer cells, and smooth muscle cells.[21,23,24] Agn has been used for spleen and liver disease, but its effects on liver fibrosis remain largely undefined. In this study, we investigated the ability of Agn to prevent the growth and proliferation of HSCs and subsequent liver fibrosis.

Materials and Methods

Chemicals

PDGF-BB was purchased from PeproTech (Shanghai, China). Alginate (Agn, A0682) was obtained from Sigma (St Louis, United States). CCl_4, ALT, LDH, Hyp and AST kits were purchased from the Nanjing Jiancheng Bioengineering (Nanjing, China). ELISA kits were purchased from Boyun Biotechnology (Shanghai, China). Primary antibodies were purchased from Cell Signaling Technologies (MA, USA). Western blot reagents were purchased from Beyotime (Shanghai, China). RT-PCR primers were purchased from Sangon Biotech (Shanghai, China). Other reagents were obtained from Takara Bio (Shiga, Japan).

HSC Culture

HSC-T6 cells (Cell Bank of Chinese Academy of Sciences) were grown in DMEM supplemented with FBS (10%) and Pen/strep (100 IU/mL) under standard tissue culture conditions (37°C, 5% CO_2).

Cell Viability and Proliferation Assays

Viability was assessed via CCK-8 assays (Dojindo Laboratories Inc.). HSC-T6s in 96 wells (~8000 cells per well) were treated with Agn (12.5, 25, 50, 100, 200 or 400 μg/mL) in media for 48 h. All assays were performed in triplicate and normalized to no-drug controls. Cells were treated with CCK-8 for 2 h and absorbances were read at 450 nm. For proliferation assays, Agn or PDGF-BB (20 ng/mL) were added to HSC-T6s for 48 h, and CCK-8 assays were performed.

Cell Colony Formation Assays

Cells were seeded into Petri dishes (60 mm, 1×10^3 cells/dish) and Agn and/or PDGF-BB (20 ng/mL) treated as described. Media was replaced every 3-days and cells were fixed in PFA after 10 d of culture. Colonies were counted following crystal-violet staining (0.1%).

LDH Assays

HSC-T6 cells (8×10^3 cells/well) were drug treated and 60 μL of LDH solution was added at room temperature. Absorbances were read at 490 nm.

Flow Cytometry

For apoptosis assessments, drug-treated HSC-T6s were EDTA treated and pelleted. Cells were resuspended and washed in 200 μL of binding buffer (Annexin V-FITC Staining kit, BD Biosciences) and Annexin-V-FITC/PI stained for 15 min. Samples were resuspended in fresh binding solution and apoptosis rates were assessed on a flow cytometer.

Cell Invasion Assessments

HSC-T6s invasion was assessed in Transwells with 8-μm pore sized chambers. DMEM containing 20% FBS was added to the outside of the chambers and cells were seeded into inserts for 48 h (4×10^4 cells/well) in DMEM plus 0.05% FBS. Cells that had invaded were fixed in 4% PFA, stained with crystal violet and counted.

Wound-Healing

Confluent HSC-T6s were wounded in culture plates using a p200 pipette tip followed by drug-treatments for 48 h. Migration into the scratch site was assessed at 0 h, 24 h and 48 h.

RT-PCR

HSC-T6 cultures (control and drug treated) were lysed in Trizol for RNA extraction, and the expression of collagen I and α-SMA mRNA were analyzed by RT-PCR. Values are relative to GAPDH and were assessed using the $2^{-\Delta\Delta Ct}$ method. Primers: *Actα2*: for 5′-TGGCCACT GCTGCTTCCTCTTCTT-3′ and rev 5′-GGGGCCAGCTT CGTCATACTCCT-3′; *Col-IαI*: for 5′-GGAGAGAGCAT GACCGATGG-3′ and rev 5′-GGGACTTCTTGAGGTT GCCA-3′.

Western Blot

HSC-T6 cells or liver tissue were lysed, resolved via SDS-page electrophoresis and transferred to PVDF membranes. Membranes were incubated in 5% milk in TBST for 90 min at room temperature to block non-specific protein-protein interactions and labeled with the indicated antibodies at 4 °C overnight. The antibodies included Collagen I, α-SMA, Bcl-2, Bax, p65, IκBα, pp65, pIκBα and GAPDH (1:1000; Cell Signaling Technology, USA). Membranes were incubated with secondary antibodies for 1 h at room temperature and proteins were visualized using the commercial ECL system. Band intensities were quantified on Bio-Rad Image Lab 4.1.

In vivo Assessments

Animal protocols were approved by the Committee of Animal Care and Use at Wenzhou Medical University. (Number: wydw2019-0570). All experiments were performed ethically following the Guidelines for the Care and Use of laboratory Animals. Male SD rats weighing 200~220 g were purchased from the laboratory animal center of Wenzhou Medical University (Wenzhou, china). Models were acclimatized for 7-d during which free access to water and food and were provided in an air-conditioned facility at 22 ± 2 °C (12-h light). Body weights were assessed twice per week.

Eighty rats were randomly divided into 5 groups (n=16): (1) Normal; (2) CCl_4; (3) CCl_4 + Colchicine (Col) (0.2mg/kg); (4) CCl_4 + Agn (100 mg/kg); (5) CCl_4 + Agn (200 mg/kg). Excluding the no-drug (normal) group, rats were treated through IP injections of CCl_4 (0.2 mL/100 g, 1:1 in olive oil), twice per week over a 12 week period. Control groups received the same volume of olive oil alone. From weeks 8 to 12, rats in the Col-treated group were intragastrically administered 0.2 mg/kg Col per day, whilst the Agn group received intragastric 100 or 200 mg/kg doses. Rats in both normal and CCl_4 groups received Saline. On the 12th week, serum and liver tissues were collected.

Serological Assays

Serum AST, ALT and hydroxyproline (Hyp) were assessed using commercial kits obtained from Nanjing Jiancheng Bioengineering. Assays were performed according to the described protocols.

ELISA Assays

IL-6, TNF-α, Laminin, type Ⅲ precollagen (PCⅢ) and hyaluronic acid (HA) levels were assessed via ELISA (Shanghai Boyun Biological Technology).

Histology

For histological assessments, livers were fixed in PFA, paraffin embedded and sectioned (5 µm). Sections were H & E or Masson's trichrome stained to visualize collagen deposition.

Immunohistochemistry

Sectioned tissues were deparaffinized and dehydrated using a gradient ethanol series. Sections were probed in retrieval solution for 25 min and microwaved. Sections were then cooled and blocked in 3% H_2O_2. Sections were labeled with anti-Collagen I or anti-α-SMA primary antibodies (1:200) at 4°C overnight and stained with the indicated secondary antibodies.

Statistical Analysis

Data analysis was performed using SPSS20.0. Data are the mean ± SD. Shapiro–Wilk test together with box plots were used to assess data normality. The differences among multi-group was analyzed by one-way ANOVA followed by post hoc analyses using the Tukey's test. Each experiment was performed in triplicate. P-values < 0.05 were deemed statistically significant.

Results

Agn Inhibits HSC-T6 Cell Proliferation

Figure 1 shows that in the presence of 12.5 to 400 µg/mL Agn for 48 h, cell viability decreased ($p<0.001$) (Figure 1A).

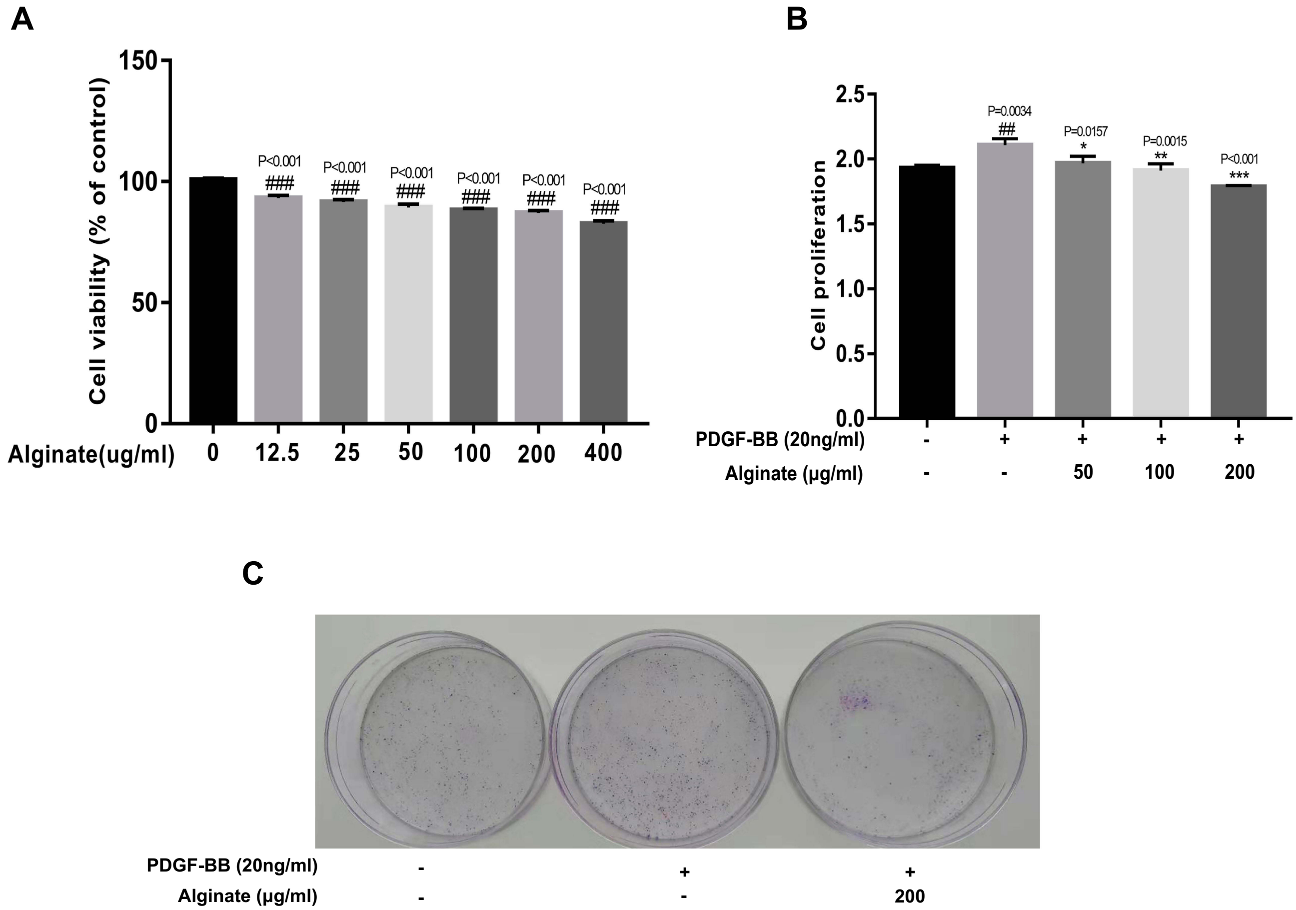

Figure 1 Agn inhibits HSC-T6 cell proliferation. (**A**) Cell viability in Agn treated cells (0, 12.5, 25, 50, 100, 200 or 400 μg/mL) assessed via CCK-8 assays. Cells were treated for 48 h. (**B**) Cell proliferation in response to Agn or PDGF-BB treatment for 48 h through CCK-8 assessments. (**C**) Effects of Agn on HSC Clonogenicity ± PDGF-BB. All experiments were repeated three times. $^{\#\#}$P<0.01, $^{\#\#\#}$P<0.001 vs normal (no-drug groups); *P<0.05, **P<0.01 and ***P<0.001 vs PDGF-BB.
Abbreviations: Agn, alginate; HSC, hepatic stellate cells; CCK-8, Cell Counting Kit-8; PDGF, platelet-derived growth factor.

We selected 50, 100 or 200 μg/mL Agn for subsequent analysis and assessed its effects on HSC-T6 cell proliferation in the presence of PDGF-BB, a known stimulator of HSCs. Figure 1B shows that three different concentrations of Agn (p=0.0157<0.05, p=0.0015<0.01, p<0.001) inhibited PDGF-BB-induced (p=0.0034<0.01) cell growth. These effects were further confirmed by colony formation assays. PDGF-BB potently enhanced colony formation, which was attenuated by Agn (Figure 1C). These results confirmed that Agn inhibits the in vitro proliferation of HSC-T6 cells.

Agn Induces HSC-T6 Apoptosis

The loss of cell membrane integrity due to apoptosis or necrosis leads to LDH release into the culture medium. LDH therefore acts as a surrogate marker of cytotoxicity. We assessed HSC-T6 viability after Agn treatment ± PDGF-BB for 48 h. We found that Agn promoted LDH release and reduced HSC viability (p<0.001), PDGF-BB does the opposite (p<0.001) (Figure 2A). Cell apoptosis in response to Agn was assessed via Annexin-V-FITC/PI staining. Agn significantly increased apoptotic rates consistent with its detrimental effects on HSC viability (p<0.001) (Figure 2B and C).

As confirmation of these findings, Bcl-2 and Bax (known indicators of apoptotic status) were assessed by Western blot in treated HSCs. The expression of Bcl-2 decreased (p=0.0404<0.05, p<0.001, p<0.001), whilst the levels of Bax increased (p<0.001, p<0.001, p<0.001) in different concentrations of Agn treated HSC-T6 cells compared to PDGF-BB treated groups (Figure 2D–F).

Agn Inhibits HSC Invasion and Migration

Wound healing assays were used to assess the effects of Agn on HSC migration and motility. Agn potently inhibited HSC-T6 cell migration (p<0.001) (Figure 3A and B). Transwell assays were used to investigate cell invasion in response to Agn. Consistent with its effects on migration,

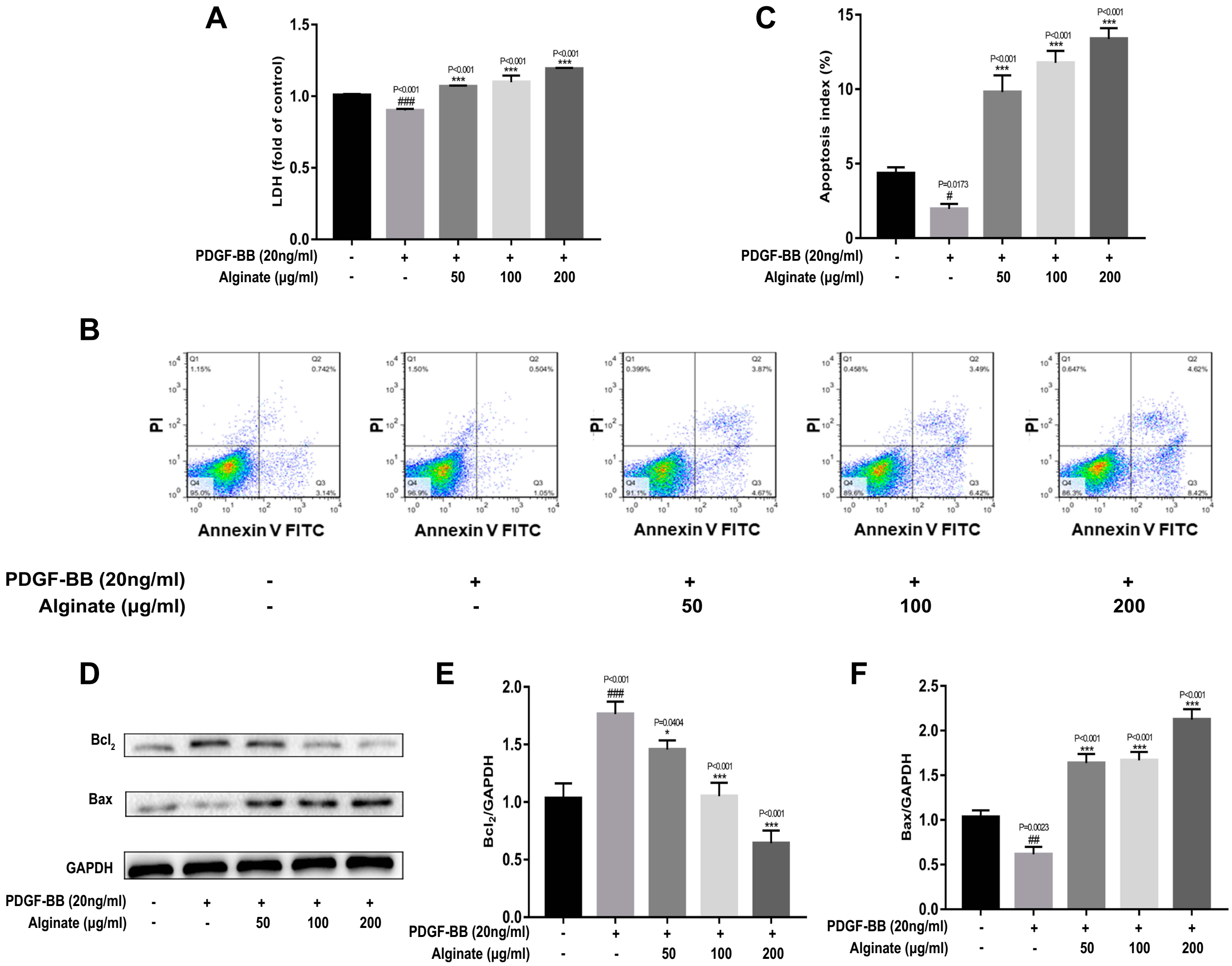

Figure 2 Agn promotes HSC apoptosis. HSC-T6s were treated with the indicated concentrations of Agn ± PDGF-BB for 48 h. (**A**) LDH assays. (**B**) Annexin V–PI stained cells. (**C**) Data quantification. (**D**) Bcl-2 and Bax expression following WB analysis (**E** and **F**) normalized to GAPDH. All experiments were repeated three times. #P<0.05, ##P<0.01 and ###P<0.001 vs normal (no-drug groups); *P<0.05 and ***P<0.001 vs PDGF-BB.

Abbreviations: Agn, alginate; HSC, hepatic stellate cells; PDGF, platelet-derived growth factor; LDH, Lactate dehydrogenase; PI, propidium iodide.

Agn treatment led to a concentration-dependent inhibition of HSC-T6 cell invasion (p<0.001) (Figure 3C and D).

Agn Prevents HSC Activation and NF-κB Signaling in HSCs

Collagen I and α-SMA are markers of HSC activation, both of which were significantly upregulated by PDGF-BB treatment (p<0.001). Importantly, these increases were attenuated by Agn (p<0.001) (Figure 4A–E).

NF-κB regulates apoptosis and cell proliferation. Figure 4C, F and G shows that NF-κB signaling decreased in response to Agn, which decreased the levels of p65 (Agn (50 μg/mL) groups versus PDGF-BB groups, p=0.0459<0.05, Agn (100 μg/mL) groups versus PDGF-BB groups, p=0.0013<0.01, Agn (200 μg/mL) groups versus PDGF-BB groups, p<0.001) and IκBα (Agn (50 μg/mL) groups versus PDGF-BB groups, p=0.0310<0.05, Agn (100 μg/mL) groups versus PDGF-BB groups, p<0.001, Agn (200 μg/mL) groups versus PDGF-BB groups, p<0.001) phosphorylation compared to PDGF-BB controls. These results suggest that Agn regulates the apoptosis and proliferation of HSCs through its effects on NF-κB signaling.

Agn Suppresses CCl_4-Induced Fibrosis and Liver Injury in vivo

Serum AST and ALT are indicators of liver damage and were investigated to evaluate hepatic injury in vivo in response to Agn. ALT and AST levels significantly increased in CCl_4 groups (p<0.001, p<0.001), whilst Agn

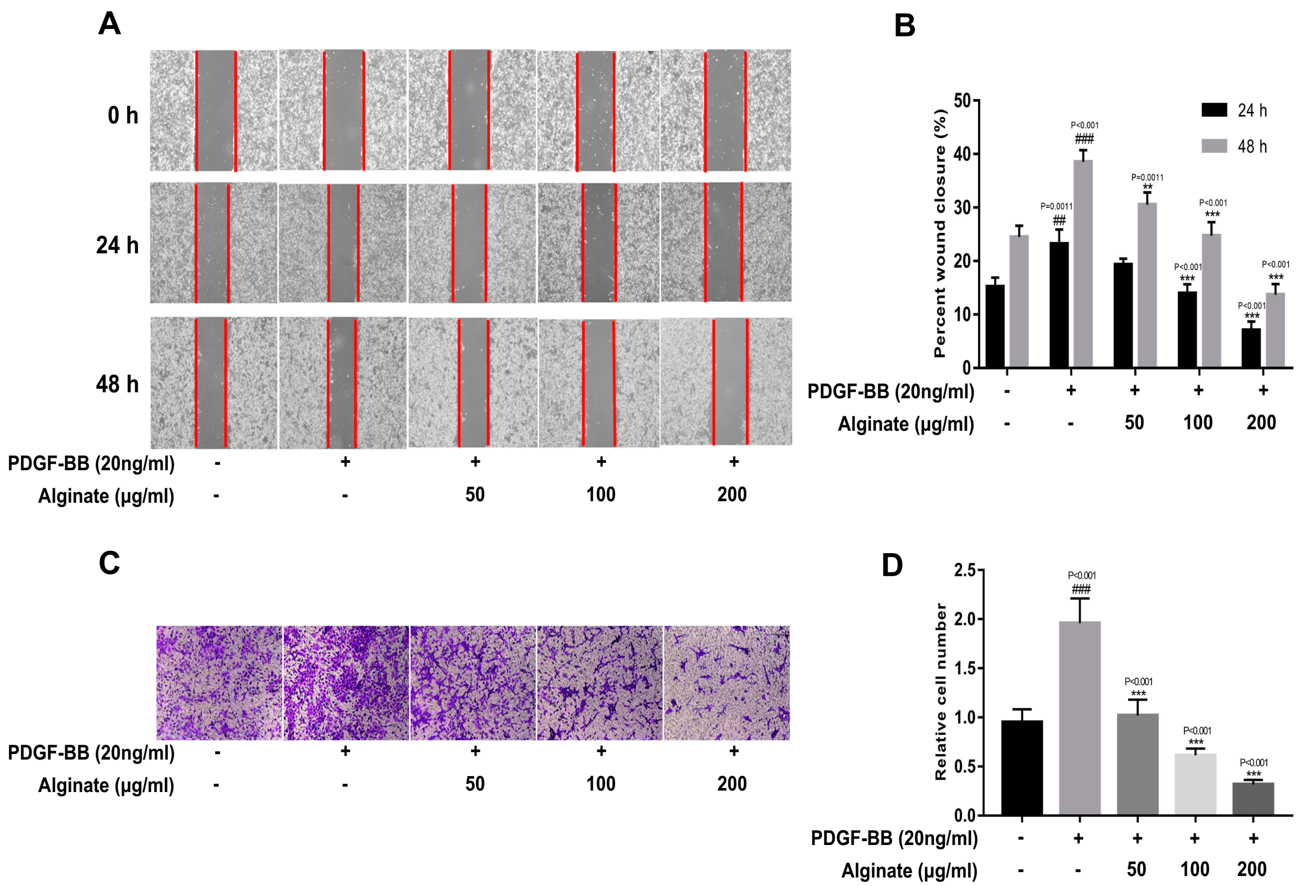

Figure 3 Agn inhibits HSC-T6 cell invasion and migration. Cells were treated as in Figures 1 and 2. (**A**) Wound healing assays. (**B**) Rates of wound healing. (**C**) Transwell assays. (**D**) Cell numbers. All experiments were repeated three times. ##P<0.01 and ###P<0.001 vs normal (no-drug groups); **P<0.01 and ***P<0.001 vs PDGF-BB.
Abbreviations: Agn, alginate; HSC, hepatic stellate cells; PDGF, platelet-derived growth factor.

(Agn (100 mg/kg) groups versus CCl_4 groups, p<0.001, p=0.0296<0.05, Agn (200 mg/kg) groups versus CCl_4 groups, p<0.001, p<0.001) and Col groups (p<0.001, p<0.001) showed a marked decrease in expression, confirming their protective effects in vivo (Figure 5A and B).

Serum Hyp is a biochemical marker of hepatic fibrosis, the levels of which significantly increased in CCl_4 in vivo models (p<0.001) (Figure 5C). H & E staining revealed that a unordered liver structure, proliferation, fibrous connective tissue and inflammatory cell accumulation in the portal region compared to CCl_4 treated groups (Figure 5D). Masson's analysis revealed extensive collagen accumulation in CCl_4 models (Figure 5E) which was alleviated through Agn and Col treatment. Fewer histopathological lesions and lower levels of liver fibrosis were also observed. Hyp levels similarly declined, confirming a protective effect.

Agn Inhibits ECM Production in vivo

Increased ECM deposition of collagen, fibronectin, laminin, and glycosaminoglycan occurs during liver fibrosis.[25] We assessed ECM production through the tissue and plasma levels of α-SMA, Collagen I, pcIII, LN and HA. α-SMA and Collagen I expression significantly decreased in Agn (p<0.001, p<0.001) and Col (p<0.001, p<0.001) treated groups compared to CCl_4 models (Figure 6A–C). The expression of the collagen biomarkers, pcIII, LN and HA also increased in CCl_4 model groups (p<0.001, p<0.001, p<0.001). However, the increased levels of these biomarkers significantly decreased in response to Agn (Agn (100 mg/kg) groups versus CCl_4 groups, p=0.0012<0.01, p=0.0130<0.05, p<0.001, Agn (200 mg/kg) groups versus CCl_4 groups, p<0.001, p<0.001, p<0.001) and Col (p<0.001, p<0.001, p<0.001) (Figure 6D–F). IHC confirmed these findings (Figure 6G–H).

Agn Inhibits NF-κB Signaling and Inflammatory Cytokine Induced Apoptosis in Rats

Figure 7A–C shows that CCl_4 significantly upregulated pp65 and pIκBα levels in liver tissue, whilst Agn or Col

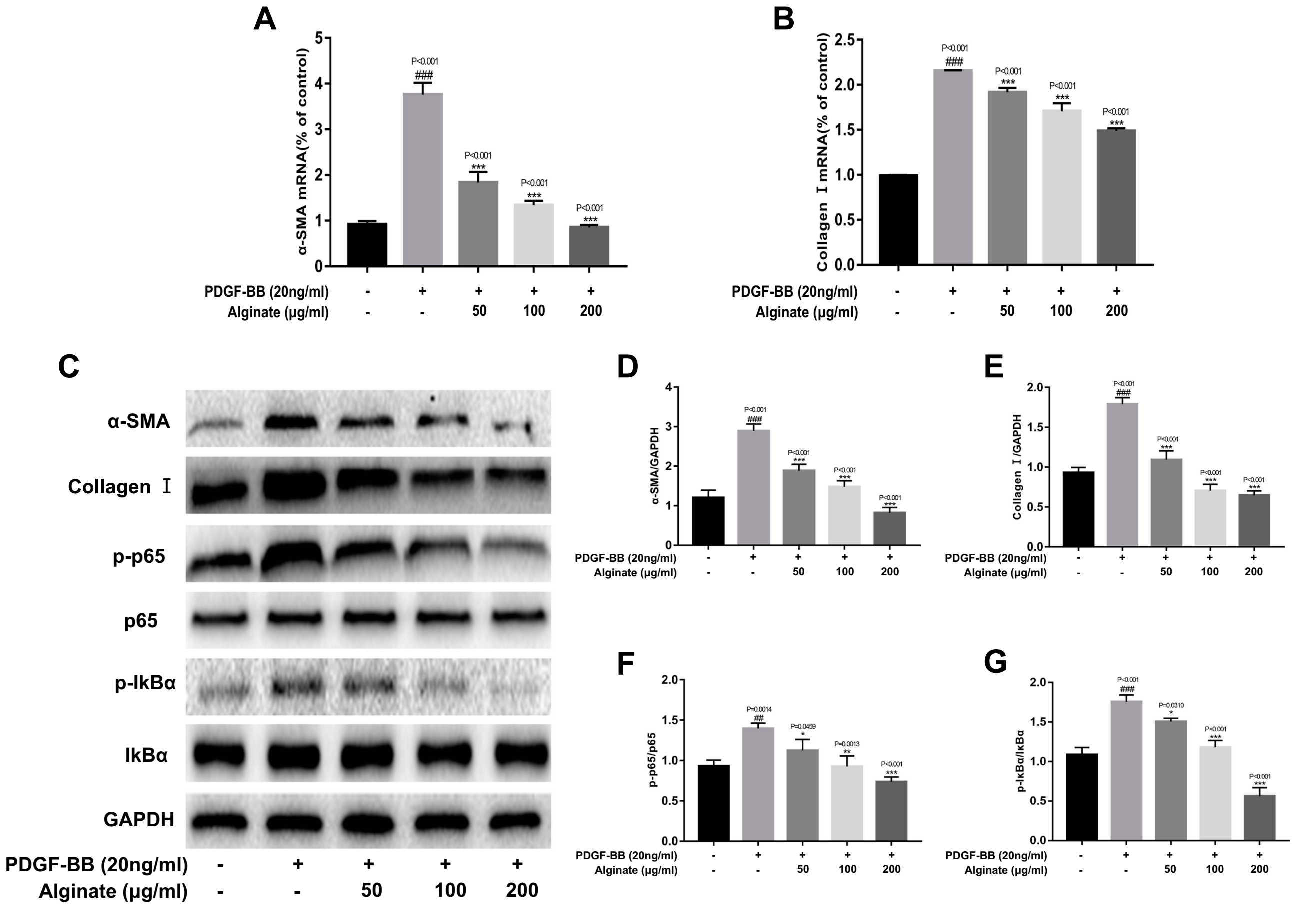

Figure 4 Agn inhibits HSC activation and NF-κB in HSCs. Cells were treated as described and α-SMA (**A**) and Collagen I (**B**) expression were investigated via q-RTPCR. (**C**) Expression of α-SMA, Collagen I, p-p65, p65, p-IκBα and IκBα by WB. Relative α-SMA (**D**) and Collagen I (**E**) levels assessed through normalization to GAPDH (loading control) in each group. Relative expression of p-p65 (**F**) and p-IκBα (**G**) through normalization to p65 and IκBα. All experiments were repeated three times. ##P<0.01 and ###P<0.001 vs normal (no-drug groups); *P<0.05, **P<0.01 and ***P<0.001 vs PDGF-BB.

Abbreviations: Agn, alginate; HSC, hepatic stellate cells; PDGF, platelet-derived growth factor; NF-κb, Nuclear factor kappa B.

remarkably reduced pp65 and pIκBα levels (p<0.001). NF-κB regulates many cellular genes/pathways including apoptosis, proliferation and Inflammation. As shown in Figure 7A, D and E, Agn (Agn (100 mg/kg) groups versus CCl_4 groups, p=0.0403<0.05, p<0.001, Agn (200 mg/kg) groups versus CCl_4 groups, p<0.001, p<0.001) and Col (p<0.001, p<0.001) significantly attenuated the induction of the anti-apoptotic protein Bcl-2, and increased Bax levels, confirming pro-apoptotic effects. Moreover, IL-6 and TNF-α levels increased in CCl_4 groups, and sharply declined in response to Agn and Col (p<0.001) (Figure 7F and G). These data suggest that Agn prevents liver fibrosis through the downregulation of NF-κB signaling.

Discussion

Liver fibrosis encompasses the scarring of healthy liver tissue that results in a loss of liver function. Fibrosis represents the first stage of liver scarring, which during later stages progresses to liver cirrhosis. Liver fibrosis is commonly caused by autoimmune hepatitis, biliary obstruction, iron overload, nonalcoholic fatty liver disease, viral hepatitis B and C, and alcoholic liver disease. During disease progression, HSC activation plays a central role. In response to chronic liver injury, resting HSCs are activated and transdifferentiate into myofibroblasts that secrete high levels of ECM that includes elastin, collagen, glycoproteins, HA and proteoglycans.[26] Preventing HSC activation therefore represents a promising treatment strategy.[27] Agn is abundant and cost-friendly, and can inhibit smooth muscle cell proliferation and fibroblast mediated collagen synthesis.[24,28,29] However, how Agn effects hepatic fibrosis has not been studied. We assessed the therapeutic effects of Agn in cultured HSCs and rat models of liver damage. We demonstrated that Agn significantly suppresses hepatic fibrosis in CCl_4-injured rats and

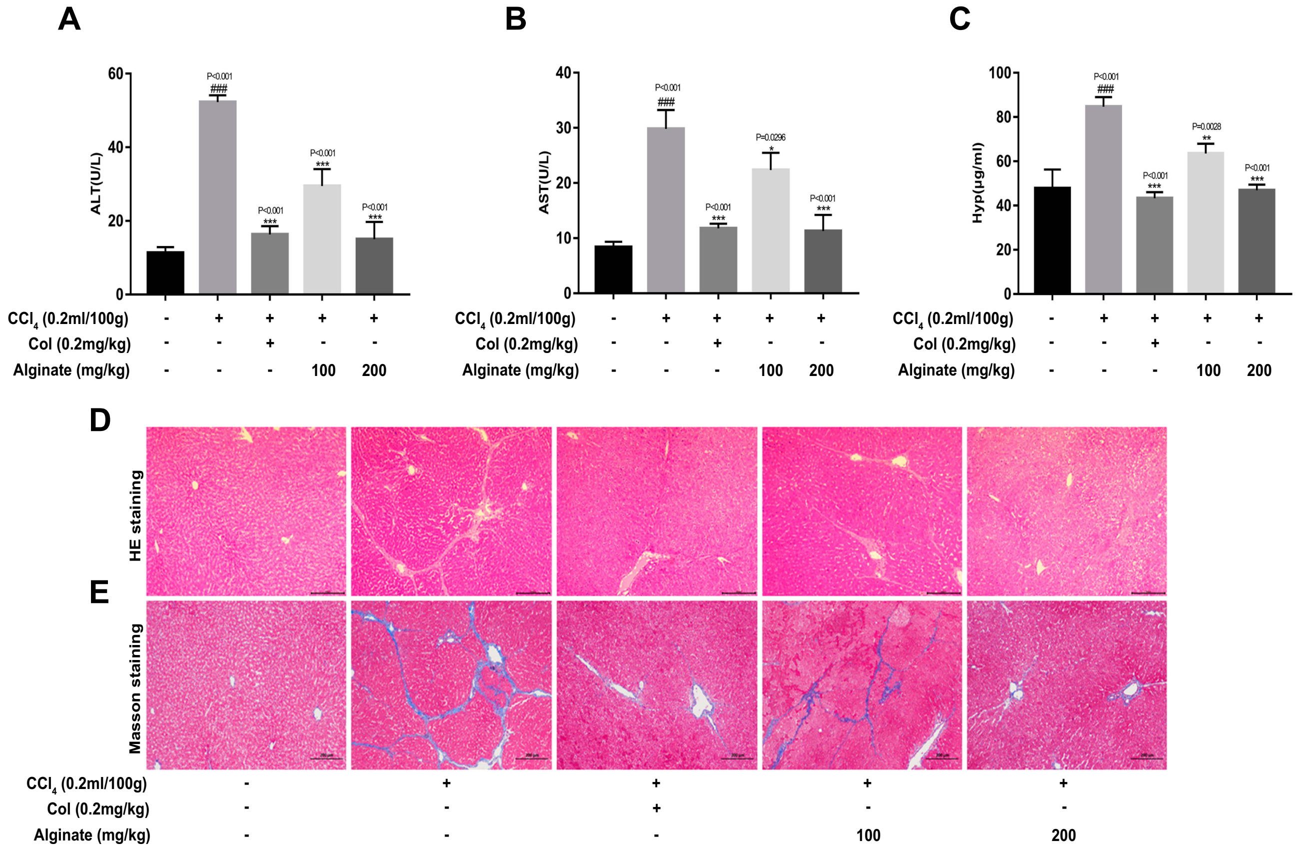

Figure 5 Agn suppresses CCl_4-induced fibrosis and liver injury in vivo. Rats were IP injected with CCl_4 (0.2 mL/100 g, 1:1 in olive oil), 2 time per week for a 12-week period. Rats received daily Agn (100 and 200 mg/kg) or Col (0.2 mg/kg) at weeks 8 to 12. ALT (**A**), AST (**B**) and Hyp (**C**) were investigated using commercially available kits. (**D**) H & E staining (magnification: × 100). (**E**) Masson's staining (Magnification, ×100). All experiments were repeated three times. ###P<0.001 vs normal (no-drug groups); *P<0.05, **P<0.01 and ***P<0.001 vs CCl_4-groups.

Abbreviations: Agn, alginate; CCl_4, carbon tetrachloride; Col, Colchicine; ALT, alanine transaminase; AST, aspartate transaminase; Hyp, hydroxyproline; H&E, hematoxylin-eosin.

inhibit HSC activation through its effects on NF-κB signaling.

Col treatment in liver fibrosis patients leads to anti-fibrotic, anti–inflammatory and immunomodulatory effects.[30] High-doses of Agn produced comparable anti-fibrotic effects. The IP injection of CCl_4 is classically used to simulate liver fibrosis.[31] Serological assessments revealed a significant increase in serum ALT and AST activity in CCl_4 model groups, indicating serious hepatocellular injury that was alleviated following Agn treatment. HE staining revealed severe histological damage in the liver tissues of CCl_4 model groups, but Agn treatment significantly attenuated these effects. Masson's staining confirmed the high levels of collagen deposition in response to CCl_4, that could be reversed by Agn. These results demonstrate that Agn attenuates CCl_4 induced liver Injury. Agn reduced HSC proliferation and LDH release from treated HSC-T6 cells demonstrated the significant cytotoxic effects of Agn to HSCs. Apoptosis is a key to the prevention of liver fibrosis.[32] To further examine the role of Agn during apoptosis, Bcl-2 and Bax expression were assessed in HSC-T6 cells and in in vivo rat models. The ratio of Bax:Bcl-2 determines apoptotic status.[33] We found that Agn significantly increased the ratio of Bax: Bcl-2, which was a potent apoptotic compound.

Liver fibrogenesis increases ECM content including collagens I, III, and IV, fibronectin, undulin, elastin, laminin, hyaluronan and proteoglycans.[7] PDGF-BB is a growth factor with multiple biological functions including the regulation of cell proliferation, viability, migration and connective tissue matrix synthesis including collagen, proteoglycans and glycosaminoglycans.[34] These findings are consistent with previous studies in which α-SMA and collagen I expression were enhanced in PDGF-BB groups compared to untreated controls. Interestingly, Agn treatment significantly decreased α-SMA and collagen I levels in HSC-T6 cells. In addition,

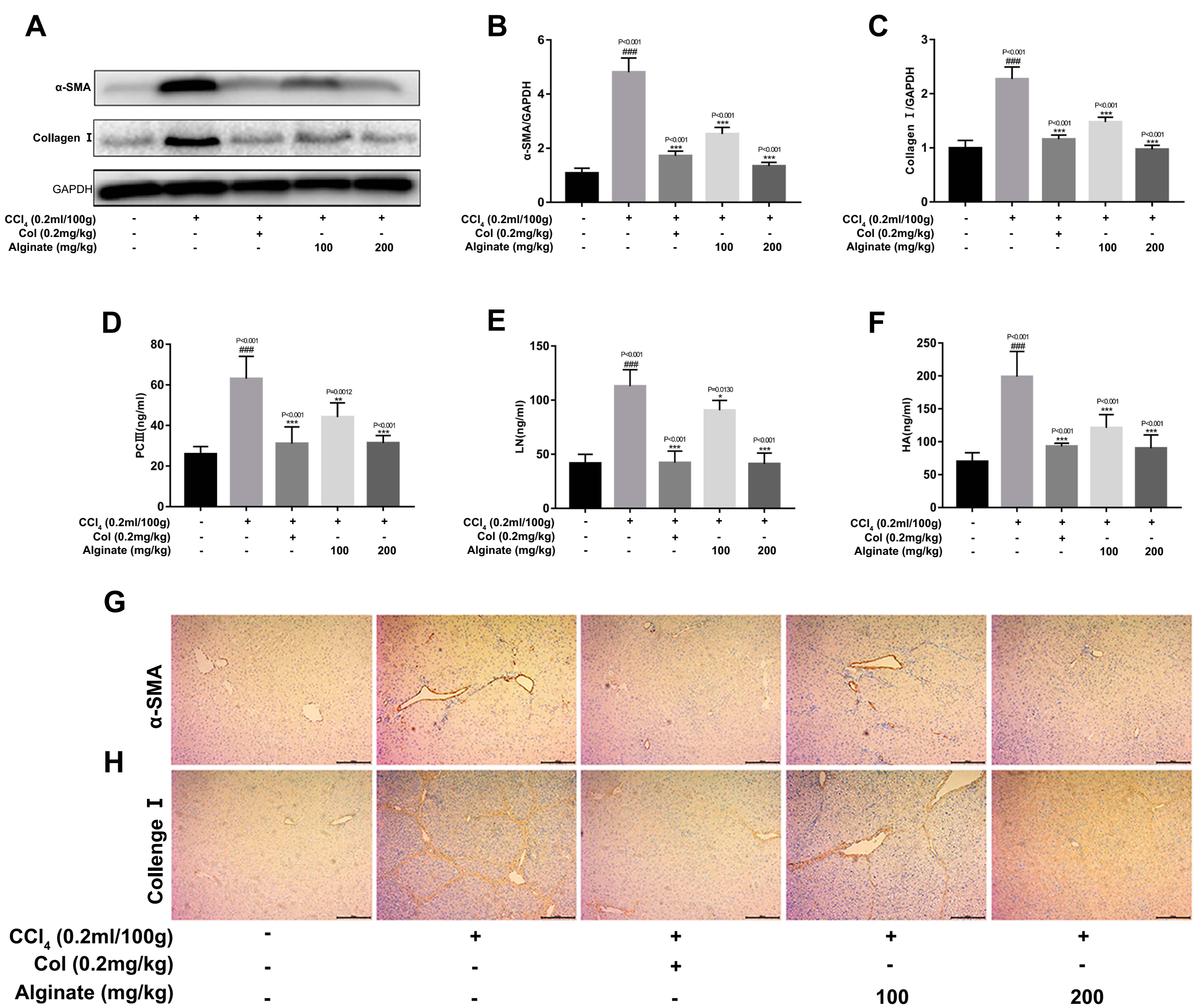

Figure 6 Agn inhibits ECM production in vivo. Rats were treated as described in Figure 5. (**A**) α-SMA and Collagen I were investigated by Western blot and normalized to GAPDH to assess relative expression levels (**B** and **C**). pcIII (**D**), LN (**E**) and HA (**F**) activity were investigated through ELISA assays. α-SMA (**G**) and Collagen expression (**H**) investigated by IHC (magnification, ×100). All experiments were repeated three times. $^{\#\#\#}$P<0.001 vs normal (no-drug groups); *P<0.05, **P<0.01 and ***P<0.001 vs CCl_4-groups.

Abbreviations: Agn, alginate; ECM, extracellular matrix; CCl_4, carbon tetrachloride; Col, Colchicine; pcIII, type III precollagen; LN, laminin; HA, hyaluronic acid; ELISA, Enzyme-linked immunosorbent assay.

Agn inhibited α-SMA and collagen I expression in CCl_4-induced rats. The levels of pcIII, LN and HA decreased after Agn treatment in CCl_4-induced rats assessed via ELISA. These results show that Agn prevents excessive ECM deposition both in vivo and in vitro.

Accumulating evidence implicates NF-κB signaling as key to HSC proliferation.[35] Aberrant NF-κB activity also leads to liver fibrosis.[36] Studies have demonstrated NF-κB inhibition promotes HSC-T6 cell death via Bcl-2 suppression.[37,38] Our finding were consistent with those of Jeong and colleagues who showed that Agn inhibits NF-κB.[39] We further showed that Agn inhibits p65 and IκBα phosphorylation. The expression of Bcl-2 also decreased, whilst Bax expression increased. Agn also inhibited NF-κB nuclear translocation[40] and the release of IL-6 and TNF-α. These results confirmed that Agn reverses liver fibrosis through NF-κB signaling.

Conclusions

We found that Agn inhibits HSC proliferation and migration and can prevent liver fibrosis through dampening NF-κB signaling. These findings highlight the potential of Agn to alleviate liver fibrosis. Further studies in human subjects are now required.

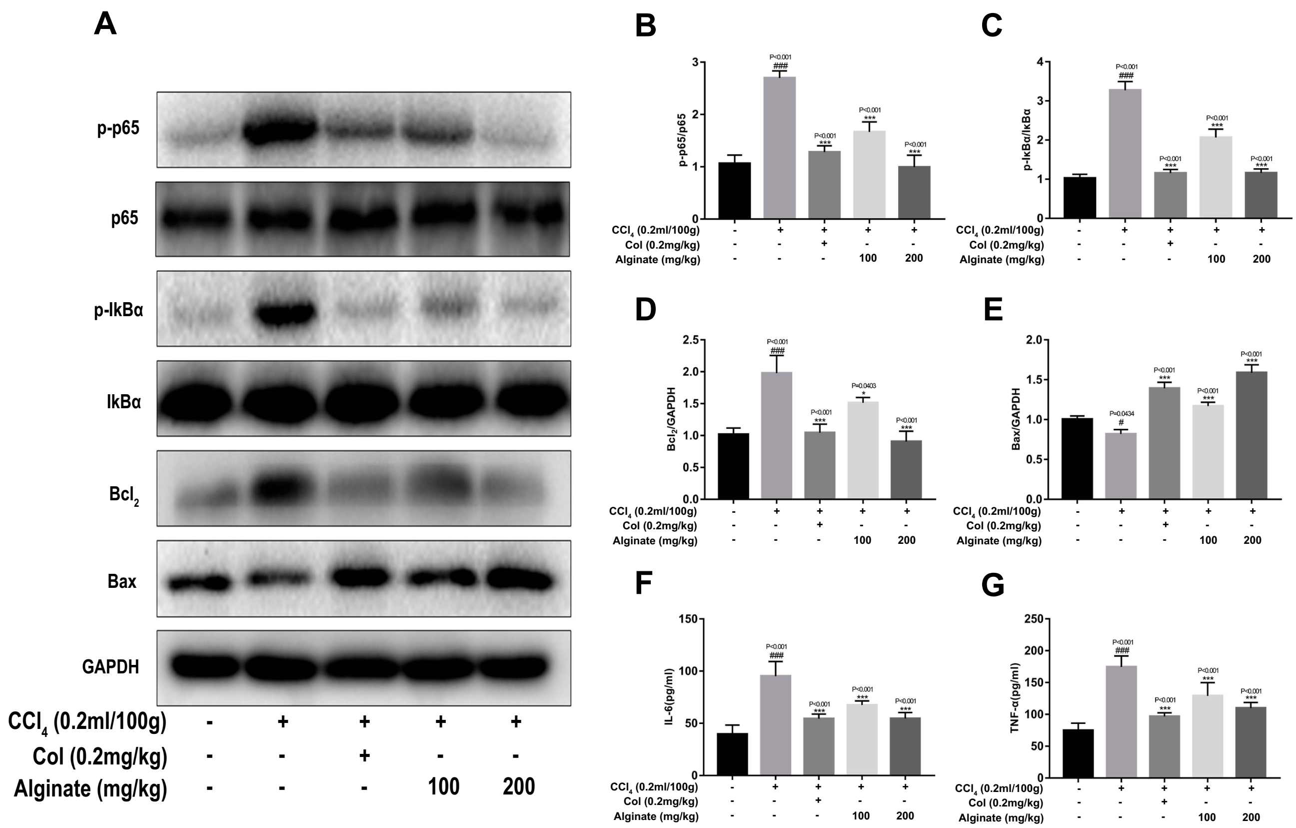

Figure 7 Agn inhibits NF-κB mediated inflammation and signaling in vivo. Rats were treated as described in Figure 5. (**A**) Expression of p-p65, p65, p-IκBα, IκBα, Bcl-2 and Bax were investigated by WB. The levels of p-p65 (**B**) and p-IκBα (**C**) were quantified through normalization to p65 and IκBα. The relative expression of Bcl-2 (**D**) and Bax (**E**) were quantified by normalizing to GAPDH. IL-6 (**F**) and TNF-α (**G**) activity were investigated by ELISA assays. All experiments were repeated three times. #P<0.05 and ###P<0.001 vs normal (no-drug groups); *P<0.05 and ***P<0.001 vs CCl_4-groups.

Abbreviations: Agn, alginate; NF-κb, Nuclear factor kappa B; CCl_4, carbon tetrachloride; Col, Colchicine; IL, interleukin; TNF, tumor necrosis factor; ELISA, Enzyme-linked immunosorbent assay.

Acknowledgments

This study was funded by the Science and Technology Bureau of Jiaxing (No. 2018AD32078) and Technology Bureau of Wenzhou (No. Y20180189).

Disclosure

The authors report no conflicts of interest in this work.

References

1. Lee UE, Friedman SL. Mechanisms of hepatic fibrogenesis. *Best Pract Res Clin Gastroenterol*. 2011;25(2):195–206. doi:10.1016/j.bpg.2011.02.005
2. Rockey DC. Translating an understanding of the pathogenesis of hepatic fibrosis to novel therapies. *Clin Gastroenterol Hepatol*. 2013;11(3):224–231.e5. doi:10.1016/j.cgh.2013.01.005
3. Blachier M, Leleu H, Peck-radosavljevic M, Valla DC, Roudot-thoraval F. The burden of liver disease in Europe: a review of available epidemiological data. *J Hepatol*. 2013;58(3):593–608. doi:10.1016/j.jhep.2012.12.005
4. Puche JE, Saiman Y, Friedman SL. Hepatic stellate cells and liver fibrosis. *Compr Physiol*. 2013;3(4):1473–1492.
5. Tome S, Lucey MR. Review article: current management of alcoholic liver disease. *Aliment Pharmacol Ther*. 2004;19(7):707–714. doi:10.1111/apt.2004.19.issue-7
6. Neuschwander-tetri BA, Wehmeier KR, Oliver D, et al. Improved nonalcoholic steatohepatitis after 48 weeks of treatment with the PPAR-gamma ligand rosiglitazone. *Hepatology*. 2003;38(4):1008–1017. doi:10.1002/hep.1840380427
7. Bataller R, Brenner DA. Liver fibrosis. *J Clin Invest*. 2005;115(2):209–218. doi:10.1172/JCI24282
8. Luedde T, Schwabe RF. NF-κB in the liver—linking injury, fibrosis and hepatocellular carcinoma. *Nat Rev Gastroenterol Hepatol*. 2011;8(2):108–118. doi:10.1038/nrgastro.2010.213
9. Oakley F, Meso M, Iredale JP, et al. Inhibition of inhibitor of κB kinases stimulates hepatic stellate cell apoptosis and accelerated recovery from rat liver fibrosis. *Gastroenterology*. 2005;128(1):108–120. doi:10.1053/j.gastro.2004.10.003
10. Moss BL, Elhammali A, Fowlkes T, et al. Interrogation of inhibitor of nuclear factor kappaB alpha/nuclear factor kappaB (IkappaBalpha/NF-kappaB) negative feedback loop dynamics: from single cells to live animals in vivo. *J Biol Chem*. 2012;287(37):31359–31370. doi:10.1074/jbc.M112.364018
11. Smidsrød O, Skjåk-braek G. Alginate as immobilization matrix for cells. *Trends Biotechnol*. 1990;8(3):71–78. doi:10.1016/0167-7799(90)90139-O

12. Yamasaki M, Moriwaki S, Miyake O, Hashimoto W, Murata K, Mikami B. Structure and function of a hypothetical Pseudomonas aeruginosa protein PA1167 classified into family PL-7: a novel alginate lyase with a beta-sandwich fold. *J Biol Chem*. 2004;279(30):31863–31872. doi:10.1074/jbc.M402466200
13. Lee KY, Mooney DJ. Alginate: properties and biomedical applications. *Prog Polym Sci*. 2012;37(1):106–126. doi:10.1016/j.progpolymsci.2011.06.003
14. Kulig D, Zimoch-korzycka A, Jarmoluk A. Cross-linked alginate/chitosan polyelectrolytes as carrier of active compound and beef color stabilizer. *Meat Sci*. 2017;123:219–228. doi:10.1016/j.meatsci.2016.08.010
15. Li J, He J, Huang Y. Role of alginate in antibacterial finishing of textiles. *Int J Biol Macromol*. 2017;94:466–473. doi:10.1016/j.ijbiomac.2016.10.054
16. Yudiati E, Isnansetyo A, Murwantoko T, Handayani CR. Alginate from *Sargassum siliquosum* simultaneously stimulates innate immunity, upregulates immune genes, and enhances resistance of Pacific white shrimp (*Litopenaeus vannamei*) against white spot syndrome virus (WSSV). *Mar Biotechnol (NY)*. 2019;21(4):503–514. doi:10.1007/s10126-019-09898-7
17. Son EH, Moon EY, Rhee DK, Pyo S. Stimulation of various functions in murine peritoneal macrophages by high mannuronic acid-containing alginate (HMA) exposure in vivo. *Int Immunopharmacol*. 2001;1(1):147–154. doi:10.1016/S1567-5769(00)00012-6
18. Hong H-J, Kim B-G, Ryu J. Preparation of highly stable zeolite-alginate foam composite for strontium(^{90} Sr) removal from seawater and evaluation of Sr adsorption performance. *J Environ Manage*. 2018;205:192–200. doi:10.1016/j.jenvman.2017.09.072
19. Wang C, Luo W, Li P, et al. Preparation and evaluation of chitosan/alginate porous microspheres/*Bletilla striata* polysaccharide composite hemostatic sponges. *Carbohydr Polym*. 2017;174:432–442. doi:10.1016/j.carbpol.2017.06.112
20. Kelishomi ZH, Goliaei B, Mahdavi H, et al. Antioxidant activity of low molecular weight alginate produced by thermal treatment. *Food Chem*. 2016;196:897–902. doi:10.1016/j.foodchem.2015.09.091
21. Cong Q, Xiao F, Liao W, Dong Q, Ding K. Structure and biological activities of an alginate from Sargassum fusiforme, and its sulfated derivative. *Int J Biol Macromol*. 2014;69:252–259. doi:10.1016/j.ijbiomac.2014.05.056
22. Marounek M, Volek Z, Skřivanová E, Taubner T, Pebriansyah A, Dušková D. Comparative study of the hypocholesterolemic and hypolipidemic activity of alginate and amidated alginate in rats. *Int J Biol Macromol*. 2017;105(Pt 1):620–624. doi:10.1016/j.ijbiomac.2017.07.077
23. Fujihara M, Nagumo T. An influence of the structure of alginate on the chemotactic activity of macrophages and the antitumor activity. *Carbohydr Res*. 1993;243(1):211–216. doi:10.1016/0008-6215(93)84094-M
24. Logeart D, Prigent-Richard S, Boisson-vidal C, et al. Fucans, sulfated polysaccharides extracted from brown seaweeds, inhibit vascular smooth muscle cell proliferation. II. Degradation and molecular weight effect. *Eur J Cell Biol*. 1997;74(4):385–390.
25. Bruckner-tuderman L, Bruckner PE. Genetic diseases of the extracellular matrix: more than just connective tissue disorders. *J Mol Med (Berl)*. 1998;76(3–4):226–237. doi:10.1007/s001090050213
26. Gressner OA, Weiskirchen R, Gressner AM. Biomarkers of liver fibrosis: clinical translation of molecular pathogenesis or based on liver-dependent malfunction tests. *Clin Chim Acta*. 2007;381(2):107–113. doi:10.1016/j.cca.2007.02.038
27. Liu Z, Yi J, Ye R, et al. miR-144 regulates transforming growth factor-β1 iduced hepatic stellate cell activation in human fibrotic liver. *Int J Clin Exp Pathol*. 2015;8(4):3994–4000.
28. Logeart D, Prigent-richard S, Jozefonvicz J, Letourneur D. Fucans, sulfated polysaccharides extracted from brown seaweeds, inhibit vascular smooth muscle cell proliferation. I. Comparison with heparin for antiproliferative activity, binding and internalization. *Eur Jo Cell Biol*. 1997;74(4):376–384.
29. Tajima S, Inoue H, Kawada A, Ishibashi A, Takahara H, Hiura N. Alginate oligosaccharides modulate cell morphology, cell proliferation and collagen expression in human skin fibroblasts in vitro. *Arch Dermatol Res*. 1999;291(7–8):432–436. doi:10.1007/s004030050434
30. Nikolaidis N, Kountouras J, Giouleme O, et al. Colchicine treatment of liver fibrosis. *Hepato-Gastroenterology*. 2006;53(68):281–285.
31. Liu JY, Chen CC, Wang WH, et al. The protective effects of Hibiscus sabdariffa extract on CCl_4-induced liver fibrosis in rats. *Food Chem Toxicol*. 2006;44(3):336–343. doi:10.1016/j.fct.2005.08.003
32. Sun M, Kisseleva T. Reversibility of liver fibrosis. *Clin Res Hepatol Gastroenterol*. 2015;39(Suppl 1):S60–S63. doi:10.1016/j.clinre.2015.06.015
33. Khan N, Afaq F, Mukhtar H. Apoptosis by dietary factors: the suicide solution for delaying cancer growth. *Carcinogenesis*. 2007;28(2):233–239. doi:10.1093/carcin/bgl243
34. Heldin CH, Westermark B. Mechanism of action and in vivo role of platelet-derived growth factor. *Physiol Rev*. 1999;79(4):1283–1316. doi:10.1152/physrev.1999.79.4.1283
35. Borghi A, Verstrepen L, Beyaert R. TRAF2 multitasking in TNF receptor-induced signaling to NF-κB, MAP kinases and cell death. *Biochem Pharmacol*. 2016;116:1–10. doi:10.1016/j.bcp.2016.03.009
36. Kang HH, Kim IK, Lee HI, et al. Chronic intermittent hypoxia induces liver fibrosis in mice with diet-induced obesity via TLR4/MyD88/MAPK/NF-kB signaling pathways. *Biochem Biophys Res Commun*. 2017;490(2):349–355. doi:10.1016/j.bbrc.2017.06.047
37. Chen G, Wang Y, Li M, et al. Curcumol induces HSC-T6 cell death through suppression of Bcl-2: involvement of PI3K and NF-κB pathways. *Eur J Pharm Sci*. 2014;65:21–28. doi:10.1016/j.ejps.2014.09.001
38. Aslan A, Gok O, Erman O, Kuloglu T. Ellagic acid impedes carbontetrachloride-induced liver damage in rats through suppression of NF-kB, Bcl-2 and regulating Nrf-2 and caspase pathway. *Biomed Pharmacother*. 2018;105:662–669. doi:10.1016/j.biopha.2018.06.020
39. Jeong HJ, Lee SA, Moon PD, et al. Alginic acid has anti-anaphylactic effects and inhibits inflammatory cytokine expression via suppression of nuclear factor-κB activation. *Clin Exp Allergy*. 2006;36(6):785–794. doi:10.1111/j.1365-2222.2006.02508.x
40. Baldwin JAS. The NF-κB and IκB proteins: new discoveries and insights. *Annu Rev Immunol*. 1996;14:649–683. doi:10.1146/annurev.immunol.14.1.649